SIMPLE SETUPS FOR CARRIER-ENVELOPE-PHASE STABLE SINGLE-CYCLE ATTOSECOND PULSE GENERATION

J. Hebling, G. Almási, J. Fülöp, M. Mechler
MTA-PTE High Field Terahertz Research Group, 7624 Pécs, Hungary
Z. Tibai, Gy. Tóth, Institute of Physics, University of Pécs, 7624 Pécs, Hungary

Abstract

A robust method for producing half-cycle—few-cycle pulses in mid-infrared to extreme ultraviolet spectral ranges is proposed. It is based on coherent undulator radiation of relativistic ultrathin electron layers (nanobunches), which are produced by nanobunching of ultrashort electron bunches by a TW power laser in a modulator undulator. According to our numerical calculations it is possible to generate shorter than 7 nm long nanobunches in this way, where the key points is to use a single-period modulator undulator, rather than a multi-period one, having an undulator parameter of only $K = 0.25$ and a significantly shorter period than the resonant period length. By using these electron nanolayers the production of carrier-envelope-phase stable pulses with up to a few nJ energy and down to 18 nm wavelength and 35 as duration is predicted.

INTRODUCTION

Waveform-controlled few-cycle laser pulses enabled the generation of isolated attosecond pulses and their application to the study of electron dynamics in atoms, molecules, and solids [1]. Intense waveform-controlled extreme ultraviolet (EUV)/X-ray attosecond pulses could enable precision time-resolved studies of core-electron processes by using e.g. pump-probe techniques [2]. Examples are time-resolved imaging of isomerisation dynamics, nonlinear inner-shell interactions, or multi-photon processes of core electrons. EUV pump–EUV probe experiments can be carried out at free-electron lasers (FELs) [3, 4]; however, the temporal resolution is limited to the fs regime and the stochastic pulse shape is disadvantageous. The shortest electromagnetic pulses reported to date, down to a duration of only 67 as, were generated by high-order harmonic generation (HHG) in gas targets [5, 6]. Isolated single-cycle 130-as pulses were generated by HHG using driving pulses with a modulated polarization state [7]. One drawback of gas HHG is the relatively low EUV pulse energy due to the ionization depletion of the medium. The use of long focal length for the IR driving field, or using strong THz fields for HHG enhancement [8] were proposed to increase the EUV pulse energy. The generation of half-cycle 50-as EUV pulses with up to 0.1 mJ energy is predicted for coherent Thomson backscattering from a laser-driven relativistic ultrathin electron layer by irradiating a double-foil target with intense few-cycle laser pulses at oblique incidence [9, 10]. Various schemes, such as the longitudinal space charge amplifier [11, 12], two-color enhanced self-amplified spontaneous emission (SASE) [13, 14], the interaction of an ultrarelativistic electron beam with a few-cycle, intense laser pulse and an intense pulse of the coherent x-rays [15], or ultraviolet laser induced microbunching in electron beams [16] were proposed for attosecond pulse generation at FELs. However, the realization of these technically challenging schemes has yet to be demonstrated and precise waveform control is difficult. In our previous work we proposed a robust method for producing half-cycle–few-cycle pulses in the MIR-EUV spectral range [17, 18]. It is based on coherent undulator radiation of relativistic ultrathin electron layers, which are produced by nanobunching of ultrashort electron bunches by a TW-power laser in a nanobuncher undulator. In this contribution we further examine this method and discuss in more detail the important findings of optimal electron nanobunching in a non-resonant undulator.

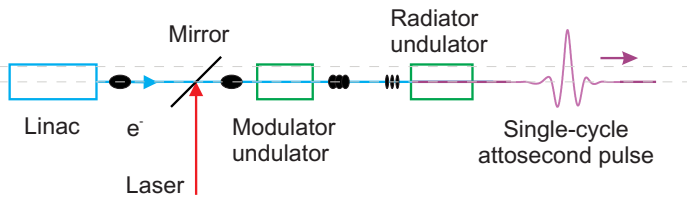

Figure 1: Scheme of the proposed setup.

SIMPLE SETUP

The proposed setup is shown in Fig. 1. The method based on ultrahin electron layer generation and subsequent coherent undulator radiation. A relativistic electron beam, e.g., from a linac is sent through a single-period modulator undulator where a TW-power laser beam is superimposed on it in order to generate nanobunches by inverse free-electron laser (IFEL) action. The nanobunched electron beam then passes through a radiator undulator consisting of a single or a few periods. The radiator undulator is placed at a position behind the modulator undulator where the nanobunch length is shortest.

Efficient ultrashort pulse generation by coherent undulator radiation is possible only if the (micro/nano)bunch length is shorter than the radiation's half period. We note that the previously reported shortest microbunch length was about 800 nm, where the beam of a CO_2 laser was used in the modulator undulator [19].

ISBN 978-3-95450-126-7

Copyright © 2013 CC-BY-3.0 and by the respective authors

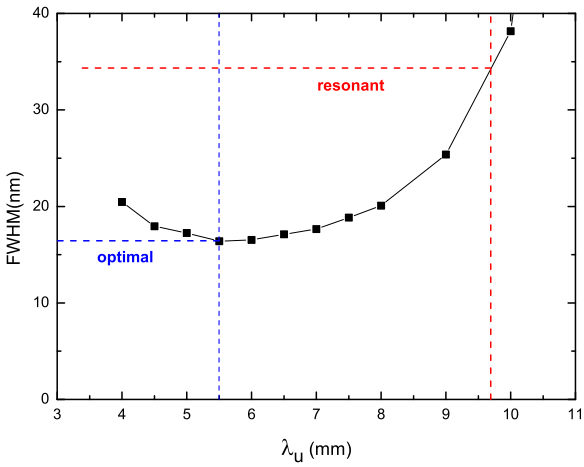

Figure 2: Dependence of the FWHM of the nanobunch on the undulator period.

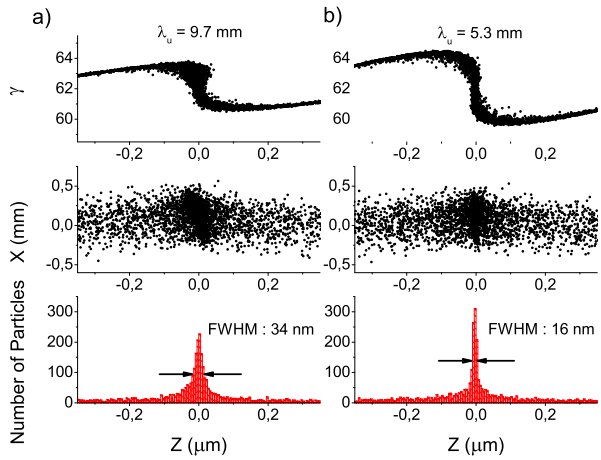

Figure 3: Snapshots of distributions of macroparticles after compression by the IFEL process. The panels show the relativistic factor γ, the spatial distribution in the $x-z$ plane, and the distribution along the z axis a) with the resonant and b) with the optimal undulator period.

PRODUCTION OF ULTRATHIN ELECTRON LAYERS BY IFEL ACTION

We used the General Particle Tracer (GPT) [20] numerical code for simulation of microbunching by inverse free electron laser (modulator or nanobuncher undulator). This code takes into account space-charge effects by using the model described in [21]. In the first simulations, we used the bunch parameters of an existing injector [22] (before the nanobunching). In order to produce shorter microbunches a laser wavelength of 1.3 μm was chosen first, the laser power was increased to 4 TW, and only a single undulator period was used. Other parameters of the setup are described below.

Optimal Versus Resonant Undulator Period Lengths

In our calculation the λ_u undulator period was first chosen to satisfy the well-known

$$\lambda_{u,r} = \frac{2\gamma^2\lambda_l}{1+K^2/2} \qquad (1)$$

resonance condition [23]. This choice of $\lambda_{u,r} = 9.7$ mm resulted in a nanobunch length of about 34 nm being already much shorter than the previously reported shortest one [19]. However, the interesting result in our simulations (with fixed considered injector parameters) is that a shorter nanobunch can be achieved by using a shorter undulator period length than the $\lambda_{u,r}$ resonant length. Figure 2 displays the calculated full width at half maximum (FWHM) values of the nanobunches as a function of the undulator period with all other parameters having fixed values. For an optimal undulator period of $\lambda_{u,o} = 5.5$ mm as short as about 16 nm electron nanobunches were obtained, which is shorter by more than a factor of two as compared to the resonant case.

The two important cases of resonant and optimal undulator periods are shown in more detail in Fig. 3. The lower part of Fig. 3 displays the histograms for the longitudinal distribution of the electrons (numerically represented by macroparticles). The FWHM widths of these distributions are 34 nm and 16 nm for the resonant and the optimal cases, respectively, as mentioned above. The middle part of Fig. 3 shows the corresponding particle distributions in the plane of the undulator. Comparison of the upper panels of Figs. 3a and 3b indicates that the main reason of the shorter nanobunch in case of the sub-resonant undulator period is the stronger modulation of the electron energy.

The reason why a shorter nanobunch length is obtained with sub-resonant undulator period can be explained in more detail by observing the work of the external (transversal) fields, i.e., that of the laser and the modulator undulator, on individual electrons (macroparticles). Figure 4 shows this work as a position inside the single-period modulator undulator. Considering electrons with nearly maximal energy gain or loss (green or blue circles in the inset of Fig. 4) in the resonant case reveals that the energy modulation reaches a maximum inside the undulator but subsequently it also gets reduced. Such a reduction is not present in case of the shorter, optimal undulator period, where the electrons leave the undulator with approximately the maximum energy modulation.

Effect of Undulator Parameter

We also analyzed the achievable minimum nanobunch length for various undulator parameter values. The result of such a series of calculations is shown in Fig. 5. The shortest nanobunches where obtained with $K = 0.25$ undulator parameter value. We note that this value is by one order of magnitude smaller than the $K = 3$ value used in

Copyright © 2013 CC-BY-3.0 and by the respective authors

ISBN 978-3-95450-126-7

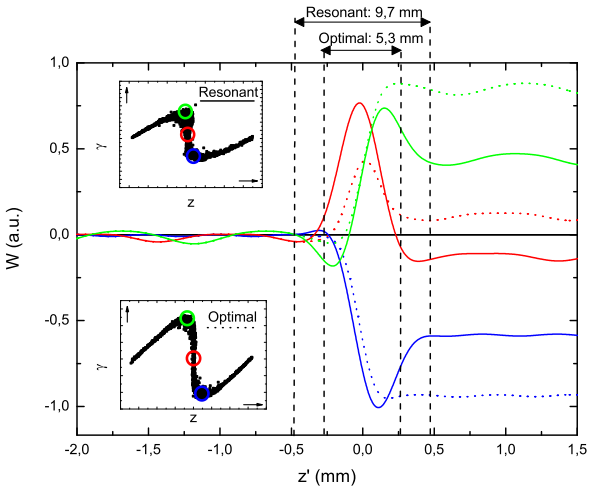

Figure 4: Work of the laser and undulator fields done on electrons with different trajectories in the optimal and the resonant cases as a position inside the single-modulator undulator. The insets show the corresponding electron energy distributions at the position of maximum nanobunch compression.

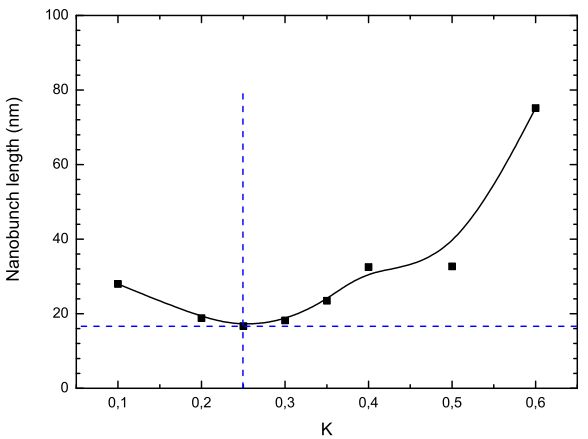

Figure 5: Dependence of the minimum nanobunch length (FWHM) on the undulator parameter.

Ref. [19]. Using such small K was essential in obtaining the extremely short nanobunches in our case. These ultrathin electron bunches allow to generate coherent undulator radiation even in the EUV spectral range. This will be discussed in the next Section.

WAVEFORM-CONTROLLED ATTOSECOND PULSE GENERATION

We used the following handbook formula to calculate the temporal shape of the electric field of the radiation generated by the ultrathin electron layers described above in a second (radiator) undulator [24]:

$$\vec{E}(\vec{r},t) = \left[\frac{q\mu_0}{4\pi} \frac{\vec{R} \times \left((\vec{R} - R\vec{\beta}) \times \dot{\vec{v}} \right)}{(R - \vec{R} \cdot \vec{\beta})^3} \right]_{\text{ret}} , \qquad (2)$$

where q is the electric charge of a macroparticle, μ_0 is the vacuum permeability, $\vec{R}$ is the vector pointing from the position of the particle at the retarded time to the observation point, $\vec{v}$ is the velocity of the macroparticle, and $\vec{\beta} = \vec{v}/c$, where c is the speed of light, and N is the number of the macroparticles. During the radiation process the acceleration, velocity, and position of the macroparticles were followed numerically by taking into account the Lorentz force equation:

$$\frac{\mathrm{d}(\gamma m \vec{v})}{\mathrm{d}t} = q\vec{v} \times \vec{B}\left(z(t)\right) , \qquad (3)$$

where $\vec{B}$ is the undulator magnetic field at the position of the macroparticle. The Coulomb interaction between the macroparticles was neglected during the radiation process. This simplification is justified by the short interaction time. The electric field was calculated in a plane perpendicular to the propagation direction of the electron nanobunch situated at 8 m behind the middle of the radiator undulator.

In a series of calculations a modulator laser with power of 10 TW and wavelength of 516 nm; and an electron bunch with $\gamma = 900$ relativistiv factor and 80 μm transversal size, and radiator undulator with a few different magnetic field distributions were assumed. The results of these calculations (see Fig. 6) indicate the versatility of the proposed method for the generation of ultrashort pulses with predefined waveforms. Pulses with a few oscillation cycles and relatively narrow spectra can be generated by an undulator consisting of a few magnetic dipole pairs. The carrier-envelope phase [25] can also be controlled by the undulator's magnetic field distribution for our attosecond pulses.

Figure 7 displays results of calculations in which the undulator parameter of the radiator undulator was kept constant at $K = 0.5$, the relativistic factor was varied in the

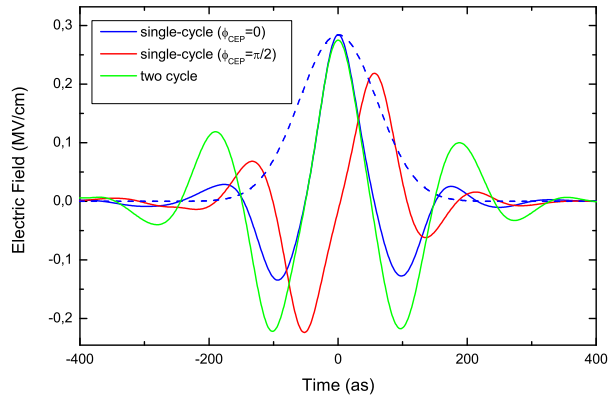

Figure 6: Examples for generated attosecond pulses with different CEP which is determined by the magnetic field distribution of the undulator. $\gamma = 900$ was assumed.

ISBN 978-3-95450-126-7

Copyright © 2013 CC-BY-3.0 and by the respective authors

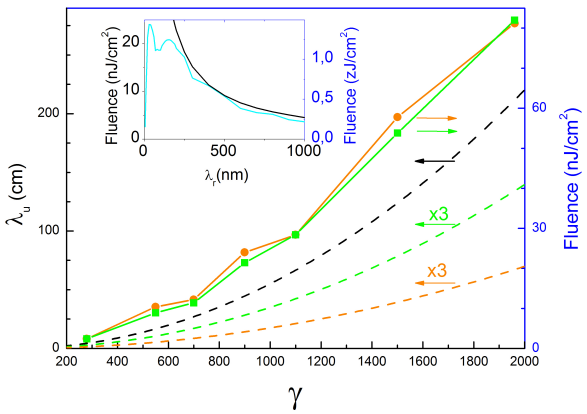

Figure 7: Dependence on γ of the generated pulse fluence for 30 nm (orange dots), and 60 nm (green squares) radiation wavelength, the needed undulator period of modulator undulator (black dash), and of radiator undulator for 30 nm (orange dash) and 60 nm (green dash). The inset shows the radiated fluence as a function of the radiation mean wavelength for the nanobunch and for a single electron.

range of $\gamma = 280 \div 2000$, and for each γ value the λ_u undulator period was chosen such that the radiation wavelength given by resonance equation becomes $\lambda_r = 30$ nm and 60 nm, respectively. At small and medium values of γ the fluence curves indicate a square dependence which is expected from a simple consideration of spatial interference [18]. At large γ values the fluence is significantly smaller than predicted by the square dependence. The reason for this is that for large γ values development of nanobunches needs as long as a few meters of drift space whereby the transverse size of the bunch increases significantly.

By using electron bunches with $\gamma = 1960$ single-cycle pulses with 0.2 nJ, 0.6 nJ and 2 nJ energy can by generated at 20 nm, 30 nm and 60 nm, respectively. These energies are high enough to use these pulses as pump in pump-probe measurements. We note that even though the radiation pulses in our setup are one order of magnitude longer than in Ref. [26], but our method is simpler and it provides perfect waveform control.

Since in our proposed setup the electron bunch consists of many nanobunches separated by the modulation laser wavelength, a pulse sequence is generated. The ratio of separation time to pulse duration, depending on the wavelength of the generated radiation and the relativistic factor, is between 20-50. The best value of 50 is reached for 35 as generated EUV pulses with mean wavelength of 18 nm. This value is 3 times larger than predicted in [26]. So we can conclude that the pulses with the predicted unique parameters can enable time- and CEP-resolved measurements with sub-100-as resolution.

We notice that there are possibilities for further increasing the ratio of pulse separation time to pulse duration significantly, for example using two modulation lasers with substantially different wavelength in the modulator undulator [14]. This might also increase the charge of the nanobunch and the energy of the generated pulses. However, investigation of this possibility and the combination of our schemes with other ones, such as the longitudinal space charge amplifier [11, 12], is out of the scope of this short article.

Another possible application of our investigated setup is seeding of FELs. Because of this we simulated generation of multi-cycle (10-cycle) attosecond pulses too. The energies of these EUV pulses are a few nJ, which is sufficient for saturating seeded FELs [27].

CONCLUSION

A robust method for producing half-cycle–few-cycle pulses in the MIR-EUV spectral range was described. It is based on coherent undulator radiation of relativistic ultrathin electron layers, which are produced by nanobunching of ultrashort electron bunches by a TW-power laser in a shorter-than-resonant single-period modulator undulator. A detailed numerical study of the nanobunching process revealed that the larger modulation of the electron energy is responsible for the shorter nanobunch length in case of the optimal sub-resonant undulator period. Nanobunches as thin as 7 nm are predicted. The temporal shape and energy of the attosecond pulses generated by such ultrathin electron layers in a radiator undulator was investigated. Carrier-envelope-phase stable pulses with up to a few nJ energy and down to 18 nm wavelength and 35 as duration are predicted.

ACKNOWLEDGMENT

This work was carried out with the financial support of the Hungarian Scientific Research Fund (OTKA, grant number 101846), and financial support of the SROP-4.2.2./B-10/2/2010-0029, SROP-4.2.1.B-10/2/KONV-2010-0002 and hELIos ELI_09-01-2010-0013 projects.

REFERENCES

[1] F. Krausz and M. Ivanov, Rev. Mod. Phys. **81**, 163 (2009).

[2] P. Tzallas et al., Nature Phys. **7**, 781 (2011).

[3] Y. Jiang et al., Phys. Rev. Lett. **105**, 263002 (2010).

[4] M. Magrakvelidze et al., Phys. Rev. A **86**, 013415 (2012).

[5] E. Goulielmakis et al., Science **320**, 1614 (2008).

[6] K. Zhao et al., Opt. Lett. **37**, 3891 (2012).

[7] G. Sansone et al., Science **314**, 443 (2006).

[8] K. Kovács et al., Phys. Rev. Lett. **108**, 193903 (2012).

[9] H.-C. Wu et al., Phys. Rev. Lett. **104**, 234801 (2010).

[10] H.-C. Wu and J. Meyer-ter-Vehn, Nature Photonics **6**, 304 (2012).

[11] M. Dohlus et al., Phys. Rev. ST Accel. Beams **14**, 090702 (2011).

[12] A. Marinelli et al., Phys. Rev. Lett. **110**, 064804 (2013).

[13] A.A. Zholents and G. Penn, Phys. Rev. ST Accel. Beams **8**, 050704 (2005).

Copyright © 2013 CC-BY-3.0 and by the respective authors

ISBN 978-3-95450-126-7

[14] Y. Ding et al., Phys. Rev. ST Accel. Beams **12**, 060703 (2009).

[15] A.A. Zholents and W.M. Fawley, Phys. Rev. Lett. **92**, 224801 (2004)

[16]]D. Xiang et al., Phys. Rev. ST Accel. Beams **12**, 060701 (2009)

[17] Z. Tibai et al., Phys. Rev. Lett., submitted

[18] Z. Tibai et al., arXiv:1304.6495

[19] W.D. Kimura et al., Phys. Rev. Lett. **92**, 05480 (2004).

[20] online at http://www.pulsar.nl/gpt

[21] G. Pöplau et al., IEEE Trans. Magn. **40**, 714 (2004).

[22] J.F. Yang et al., Jap. J. Appl. Phys. **44**, 12 (2005).

[23] P. Schmüser, M. Dohlus, J. Rossbach, "Ultraviolet and soft X-ray free-electron lasers", Springer (2008).

[24] J.D. Jackson: Classical Electrodynamics 3rd ed., Wiley, ISBN 0-471-30932-X

[25] A. Baltuska et al., Nature Phys. **421**, 611 (2003).

[26] D.J. Dunning, Phys. Rev. Lett. **110**, 104801 (2013)

[27] S. Ackermann et al., "Optimization of HHG seeding at FLASH II", FEL2012, August 2012, TUPD11

Copyright © 2013 CC-BY-3.0 and by the respective authors

ISBN 978-3-95450-126-7